Capacitance-Voltage Characteristics

of Metal-Oxide-Strained Semiconductor Si/SiGe Heterostructures

Nicolas Cavassilas, Jean-Luc Autran

Laboratoire Matériaux et Microélectronique de Provence (L2MP, UMR CNRS 6137)
Bâtiment IRPHE, 49 rue Joliot-Curie, BP 146 13384 Marseille, France
cavassil@newsup.univ-mrs.fr

ABSTRACT

We present theoretical investigation of mechanical strain-induced effects in metal-oxide-semiconductor (MOS) structures from an electrical point-of-view. In this work, we start by calculating of the strained semiconductor band-structure using a **k** . **p** approach over the complete Brillouin zone for the conduction and valence bands. The present method has been applied to silicon strained on an unstrained [001] $Si_{1-x}Ge_x$ buffer surface. The resulting carrier effective masses, energy split and energy bandgap deduced from the strained Si band-structure have been introduced in a one-dimensional solver of the Schrödinger and Poisson equations. Self-consistent calculation of the capacitance-voltage (C-V) curves has been then performed for *n*+-poly/SiO_2/*p*-Si/$Si_{1-x}Ge_x$ structures with Ge content x ranging from 0 up to 0.5. Our results highlight a strain dependence of the threshold voltage of the MOS structure due to the energy bandgap reduction and a non-linear strain effect in accumulation due to the degeneracy in the valence band.

Keywords: strain, band-structure, strained Si, SiGe, **k** . **p** theory, Schrödinger and Poisson equations, capacitance-voltage (C-V) characteristic.

1 INTRODUCTION

In Si-Ge based Metal-Oxide-Semiconductor (MOS) heterostructures, mechanical strain is considered as an essential parameter for band-structure engineering. Indeed, it offers the possibility to change the semiconductor band-structure by lowering the lattice symmetry [1]. One of the most commonly used strain-induced effects is the carrier effective masses reduction to enhance carrier mobility and, consequently, to improve dynamical performances of devices using a strained layer in their active area [2]. On the electrical point-of-view, strain-induced effects on semiconductor band-structure and lattice symmetry may have other surprising indirect consequences, for example, investigated in this work, the modification of the capacitance-voltage response (C-V) of MOS capacitors for which the semiconductor is strained. For a complete and rigorous calculation of strain-induced effects on device electrical properties, the knowledge of the strained semiconductor band-structure is required. In this paper, we present, in section 2.1, the **k** . **p** approach developed to calculate the band-structure of a strained semiconductor. The resulting extracted effective masses, energy split and energy band-gap are also reported for the particular case of strained silicon (section 2.2). In a second time, these sets of data have been introduced in a one-dimensional solver of the Schrödinger and Poisson equations to evaluate the capacitance response of MOS structures based on the Si/$Si_{1-x}Ge_x$ system. Modeling and calculation details related to this self-consistent approach are given in section 3.1. The strain dependence of such C-V curves is finally analyzed in section 3.2.

2 BAND-STRUCTURE CALCULATION

2.1 k . p approach

The initial step of this work concerns the band-structure calculation of a strained semiconductor. In this goal, we used an original *sps** **k** . **p** method [3] which allows us to calculate the energy bands all over the Brillouin zone. Schematically, to solve the Schrödinger equation in a semiconductor submitted to a biaxial [001]-strain, we consider the total Hamiltonian $H = H_{20} + H_{strain}$ where H_{strain} is the strain Hamiltonian and H_{20} is a twenty-band **k** . **p** Hamiltonian taking into account the spin-orbit coupling [3]. H_{20} is used to describe the valence band as well as the two first conduction bands. This Hamiltonian is valid for both direct and indirect bandgap semiconductors. In this study, we focused on the properties of [100]-biaxially strained Si (Fig. 1) characterized by a lateral lattice constant $a_{//}(x)$ equal to the bulk lattice constant $a_{SiGe}(x)$ of an unstrained $Si_{1-x}Ge_x$ substrate. The lattice constant $a_{\perp}(x)$ in the direction perpendicular to the interface is adapted so as to minimized the elastic energy:

$$a_{\perp}(x) = a_{Si}\left[1 - 2\frac{C_{12}}{C_{11}}\frac{a_{//}(x) - a_{Si}}{a_{Si}}\right] \quad (1)$$

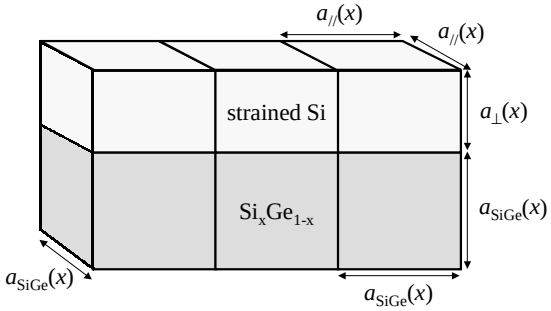

Figure 1: Schematic representation of the $Si/Si_{1-x}Ge_x$ strained system investigated in this work.

where a_{Si} is the Si bulk lattice constant and C_{11} and C_{12} are the Si elastic constants.

From the values of $a_{\perp}$, $a_{//}$ and a_{Si}, the symmetric strain tensor elements can be evaluated as follows: $\varepsilon_{xx} = \varepsilon_{yy} = \varepsilon_{//} = (a_{//} - a_{Si}) / a_{Si}$, $\varepsilon_{zz} = \varepsilon_{\perp} = (a_{\perp} - a_{Si}) / a_{Si}$ and $\varepsilon_{xy} = \varepsilon_{xz} = \varepsilon_{yz} = 0$. This biaxial strain induces two major changes in the Si band-structure. On one hand, the hydrostatic stress causes a forbidden band-gap energy shift; on the other hand, the uniaxial stress produces an additional splitting of the degenerate levels by lowering the lattice symmetry. In H_{strain}, these two components are taken into account via two sets of deformation potential parameters, (a_v, a_c) for the hydrostatic and (b_v, b_c) for the uniaxial components respectively (indexes c et v respectively refer to valence and conduction bands). For example, for the triply degenerate $\Gamma_{5c,v}$ bands ($\Gamma_8^{1/2}$, $\Gamma_8^{3/2}$ and Γ_7 states for valence and conduction bands, see Figs. 2 and 3), the strain Hamiltonian matrix takes the form:

$$\begin{array}{ccc} \Gamma_8^{3/2} & \Gamma_8^{1/2} & \Gamma_7 \\ \begin{bmatrix} a\varepsilon + b\varepsilon_{//\perp} & 0 & 0 \\ 0 & a\varepsilon - b\varepsilon_{//\perp} & \sqrt{2}b\varepsilon_{//\perp} \\ 0 & \sqrt{2}b\varepsilon_{//\perp} & a\varepsilon \end{bmatrix} & \end{array} \qquad (2)$$

where $\varepsilon = 2\varepsilon_{//} + \varepsilon_{\perp}$ and $\varepsilon_{//\perp} = \varepsilon_{\perp} + \varepsilon_{//}$. A detailed description of this model can be found in Ref. [4]. The extracted results of energy band-gap and band-splitting have been found in very good agreement with experimental data, that confirms the validity of the present approach [4].

2.2 Strained Si on [001] $Si_{1-x}Ge_x$

The calculated band-structures of unstrained Si and strained Si on [001] $Si_{0.7}Ge_{0.3}$ surface are shown in Figs. 2 and 3. The principal consequence of the biaxial [001]-strain is a conduction band-splitting into the four equivalent in-plane valleys Δ_4 and the two valleys Δ_2 along the growth direction [001]. The corresponding Δ_2 and Δ_4 band-edge energy levels as a function of Ge content are given in Fig. 4a. A direct consequence of this splitting is that electrons are principally localized, under strain, in the Δ_2 valley at thermal equilibrium. Even if the variation of the electron band-edge "curvature" effective mass, defined as the derivative of the $E - k^2$ curve when $E \to 0$, is rather limited (see Fig. 4b), another consequence of this splitting is a significant variation of the "carrier concentration" effective mass. As a result, the energy distribution of electrons in a strained MOS structure should be slightly impacted by such a mass variation.

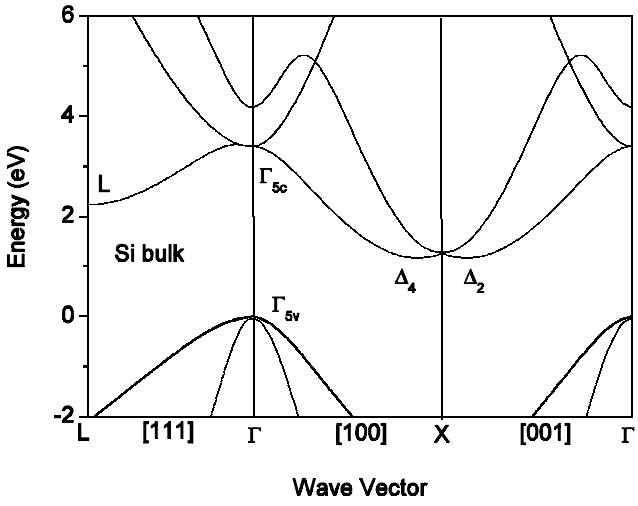

Figure 2: Calculated band-structure of unstrained silicon. Note the triply degenerated state (Γ_5) of the valence and conduction bands and the energy position of the Δ valley (Δ_2 and Δ_4) in conduction band.

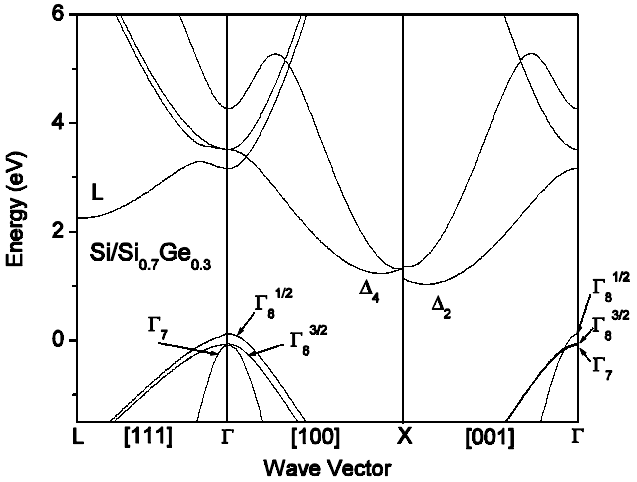

Figure 3: Calculated band-structure of strained Si on [001] $Si_{0.7}Ge_{0.3}$ surface (unstrained buffer). The biaxial [001]-strain lifts the degeneracy in conduction band Δ valley (Δ_2 and Δ_4) as well as in the valence band Γ_8 ($\Gamma_8^{1/2}$ and $\Gamma_8^{3/2}$). The fundamental energy band-gap is defined by the energy between Δ_2 and $\Gamma_8^{1/2}$ because of the tensile strain.

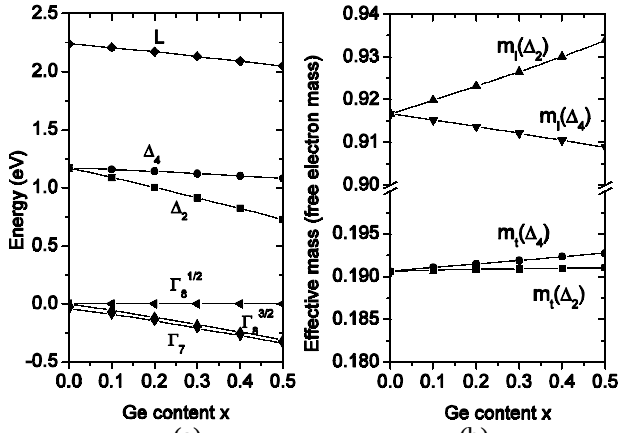

(a) (b)

Figure 4: Calculated variation of (a) the relevant conduction and valence bands and of (b) the longitudinal and transverse effective masses at the Δ_2 and Δ_4 minima in Si grown on an unstrained [001] $Si_{1-x}Ge_x$ surface as a function of Ge content x. For the energy band nomenclature, see Fig. 3.

Concerning the valence band, application of strain lifts the degeneracy in the Γ_{5v} band. In the particular case of the $Si/Si_{1-x}Ge_x$ system, i.e. in the case of a tensile strain, the energy position of $\Gamma_8^{1/2}$ band, commonly labeled "light-hole" band in unstrained Si, shifts above than the one of the $\Gamma_8^{3/2}$ band ("heavy-hole" band). Moreover, in a strained semiconductor, the concept of light and heavy hole bands loses its sense because the light or heavy character of a band is direction-dependent. This aspect in illustrated in Fig. 3 as a result of a strain in the valence band: one can observe a strong anisotropy between the in-plane and the growth directions.

Finally, these splits and energy shifts of the conduction and valence bands lead to a significant change in the energy band-gap defined as the energy interval between the Δ_2 valley and the $\Gamma_8^{1/2}$ valence band (see Fig. 4a). The impact of this band-gap as well as the effective masse strain-dependences on the electrical response of MOS structures is evaluated from a capacitance point-of-view in the next section.

3 STRAINED-SILICON BASED MOS DEVICES: C-V MODELING AND SIMULATION

3.1 Schrödinger and Poisson equations

The previously calculated carrier effective masses and energy band-gap have been introduced in a one-dimensional solver of the Schrödinger and Poisson equations in order to evaluate the impact of mechanical strain on C-V characteristics of MOS structures. Briefly, the calculation of the eigenenergies (E_{ij}) and the envelope wave-functions (Ψ_{ij}) of carriers confined in the quantum-well formed by the band bending of the silicon-oxide system (see Fig. 5) requires to solve the time-independent, effective-mass and one-dimensional Schrödinger equation:

$$-\frac{\hbar^2}{2}\frac{d}{dx}\left(\frac{1}{m_j^*(x)}\frac{d}{dx}\right)\Psi_{ij}(x)+V(x)\Psi_{ij}(x)=E_{ij}\Psi_{ij}(x) \qquad (3)$$

where $\hbar$ is the reduced Planck constant, m_j^* is the carrier effective mass, V is the carrier potential energy, subscript *i* denotes the energy sub-band (*i*=1,2,3…), subscript *j* denotes the semiconductor valley and *x* is the spatial coordinate along the direction perpendicular to the Si/SiO_2 interface. In a MOS structure, the potential energy *V* is linked to the electrostatic potential ϕ via the relation $V(x) = -q\phi(x)+\Delta E_C(z)$ where $\Delta E_C(z)$ is the silicon-oxide band offset. ϕ verifies the Poisson equation:

$$\frac{d}{dx}\left(\varepsilon(x)\frac{d}{dx}\right)\phi(x)=-\frac{q}{\varepsilon_0}\left\{p(x)-n(x)+N_D^+(x)-N_A^-(x)\right\} \qquad (4)$$

where $q\phi(x) = E_i(x) - E_F$, E_F is the Fermi level, $E_i(x)$ is the intrinsic Fermi level at the *x* coordinate, ε is the dielectric constant, ε_0 is the permittivity of vacuum, *q* is the absolute value of electron charge, *n* and *p* represent the free electron and hole densities, respectively, N_D^+ and N_A^- are the ionized acceptor and donor concentrations, respectively.

Eqs. (3) and (4) have been discretized using a three-point finite difference scheme with a non-uniform mesh in the direction perpendicular to the interface (Fig. 5). Additional numerical details about the implementation of this self-consistent solving can be found in Ref. 5.

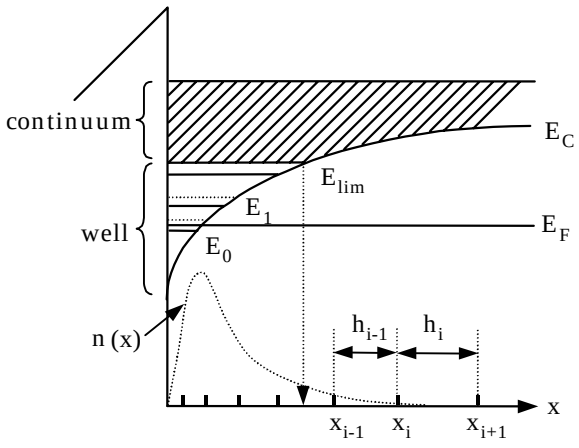

Figure 5. Energy band diagram of a n-type MOS structure in accumulation regime showing the partition of electrons into two distinct populations as a function of their energy E: electrons confined in the well ($E < E_{lim}$) and electrons distributed in the conduction band continuum ($E > E_{lim}$).

3.2 Capacitance-Voltage curves

As a result, calculated C-V curves from the above data are shown in Fig. 6 for both *n*+-poly/SiO_2/*p*-Si/$Si_{0.7}Ge_{0.3}$ and *n*+-poly/SiO_2/*p*-Si/$Si_{0.5}Ge_{0.5}$ capacitors. These curves are compared to the "reference" one related to an unstrained system. One can observe that strain significantly impacts the characteristics, especially in inversion regime. For strained MOS transistors, a direct consequence is that the threshold voltage should decrease when increasing the strain in the growth direction. We show that this effect is mainly due to the reduction of the energy band-gap with strain, as evidenced in Fig. 7. The bulk potential $\Phi_F = E_{Fi} - E_F$, which is directly related to the threshold voltage, is found to linearly decrease with strain. This behavior is due to the linear dependence of the energy band-gap with strain (Fig. 4) and to the strain-independent character of the Fermi level which only depends on the concentration of ionized impurities in Si. Note that in our model the Fermi level has been calculated by solving the electro-neutrality equation.

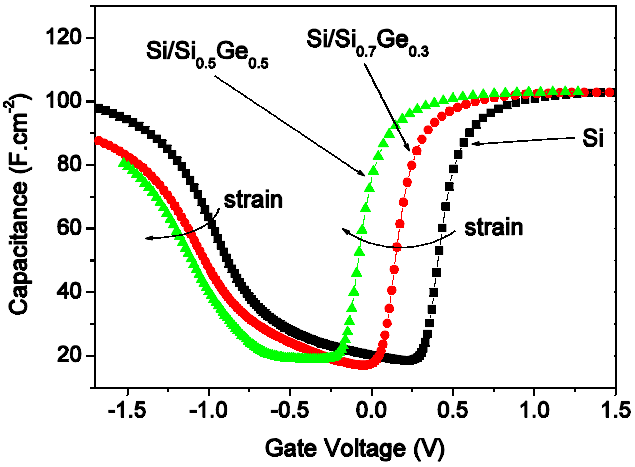

Figure 6: Simulated C-V curves of a n^+-poly/SiO_2/p-Si/ $Si_{1-x}Ge_x$ capacitor for x = 0 ("reference" unstrained system), x = 0.3 and 0.5. Other simulation parameters are: oxide thickness 27 Å, substrate doping level 5×10^{17} cm^{-3}, gate doping level 2×10^{20} cm^{-3}, flat-band voltage -1.02 V.

In accumulation regime, strain induced-effect on C-V characteristics is attributed to a strong modification of the hole effective mass in the growth direction. Indeed, as illustrated in Fig. 3, the $\Gamma_8^{1/2}$ valence band is very "inclined" in this direction. For example, the band-edge effective mass extracted from this $\Gamma_8^{1/2}$ band in the [001]-direction is ~0.35×m_0 in unstrained Si whereas this mass is reduced to ~0.12×m_0 in the Si/$Si_{0.7}Ge_{0.3}$ system. In the same time, this effective mass does not change with strain when considering the [100]-direction. Note that, contrary to the inversion case, strain-induced effect on the C-V response in accumulation is not proportional to strain. This should seriously impact the oxide thickness extraction [5] from C-V data in a strain-silicon based MOS capacitor.

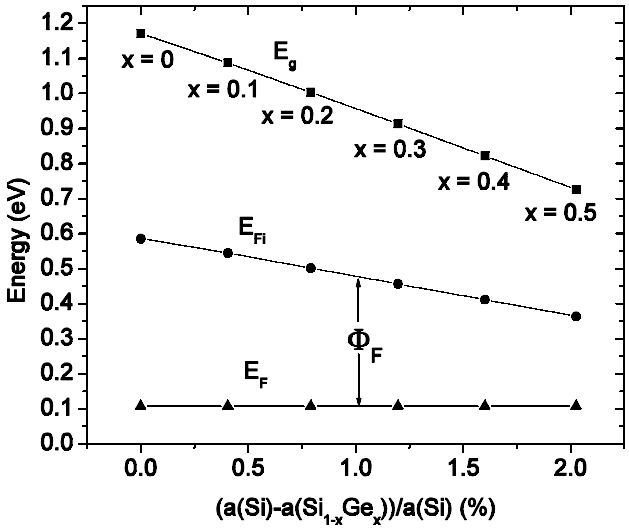

Figure 7: Energy band-gap E_g, intrinsic Fermi level E_{Fi} and Fermi level E_F versus the difference between the lattice constants of Si and $Si_{1-x}Ge_x$. E_F, calculated by solving the electro-neutrality equation, does not change with strain.

4 CONCLUSION

In summary, we have presented a theoretical work concerning strain induced-effects in Si/$Si_{1-x}Ge_x$ based MOS devices. This first study focused on the calculation of the capacitance-voltage response of such structures taken into account a strain-dependent realistic band structure for the active silicon layer. From the present analysis, we evidenced two major strain-induced effects: the first one is a strain linear decrease of the threshold voltage due to the reduction of the energy band-gap. The second one affects the accumulation regime and is due to the degeneracy lift of the Γ_{5v} valence band induced by strain. These two effects should be carefully considered in the interpretation of C-V data as well as in electrical parameter extraction related to strained-semiconductor MOS devices.

REFERENCES

[1] G. L. Bir, G. E. Pikus, Symmetry and Strain-Induced Effects in Semiconductors, John Wiley & Sons, New York/Toronto 1974.

[2] G. Höck, T. Hackbarth, N. Käb, H.-J. Herzog, M. Enciso, F. Aniel, P. Crozat, R. Adde, E. Kohn, U. König Electronic Letters, Vol 36, 1428 (2000).

[3] N. Cavassilas, F. Aniel, K. Boujdaria, G. Fishman, Phys. Rev. B 64, 115207 (2001).

[4] N. Cavassilas, F. Aniel, G. Fishman, ICCN 2002.

[5] C. Raynaud, J. L. Autran, P. Masson, M. Bidaud, A. Poncet, Mat. Res. Soc. Symp. Proc., Vol. 592, 159 (2000).